DISTINCT MUTATIONAL SIGNATURES ARE ASSOCIATED WITH CORRELATES OF INCREASED IMMUNE ACTIVITY IN PANCREATIC DUCTAL ADENOCARCINOMA

Ashton A Connor, MD[1,2,3]; Robert E Denroche[1,4], MSc; Gun Ho Jang[1,4], PhD; Lee Timms[1,5], MSc; Sangeetha N. Kalimuthu[1], MD; Iris Selander[2], MSc; Teresa McPherson[2], MSc; Gavin W. Wilson[1,4], PhD; Michelle A. Chan-Seng-Yue[1], BSc; Ivan Borozan[4], PhD; Vincent Ferretti[4], PhD; Robert C. Grant[1,2], MD; Ilinca M. Lungu, MSc[6]; Eithne Costello[7], PhD; William Greenhalf[7], PhD; Daniel Palmer[7], PhD; Paula Ghaneh[7], PhD; John P. Neoptolemos[7], MD; Markus Buchler[8], MD; Gloria Petersen[9], MD; Sarah Thayer[10], MD, PhD; Michael A. Hollingsworth[11], PhD; Alana Sherker[2,12], BSc; Daniel Durocher[2,12], PhD; Neesha Dhani[13], MD; David Hedley[13], MD; Stefano Serra[3], MD; Aaron Pollett[2,15], MD; Michael H.A. Roehrl[1,14,15,16,17], MD,PhD; Prashant Bavi[1], MD; John M.S. Bartlett[6], Sean Cleary[1,3], MD; Julie M. Wilson[1], PhD; Ludmil B. Alexandrov[18,19], PhD; Malcolm Moore[13], MD; Bradly G. Wouters[15], PhD; John D. McPherson[5,16], PhD; Faiyaz Notta[1], PhD; Lincoln D. Stein[4,12], MD, PhD; Steven Gallinger[1,2,3], MD

[1]PanCuRx Translational Research Initiative, Ontario Institute for Cancer Research, Toronto, Ontario, Canada.
[2]Lunenfeld-Tanenbaum Research Institute, Mount Sinai Hospital, Toronto, Ontario, Canada.
[3]Hepatobiliary/pancreatic Surgical Oncology Program, University Health Network, Toronto, Ontario, Canada.
[4]Informatics and Bio-computing Program, Ontario Institute for Cancer Research, Toronto, Ontario, Canada.
[5]Genome Technologies Program, Ontario Institute for Cancer Research, Toronto, Ontario, Canada.
[6]Transformative Pathology, Ontario Institute for Cancer Research, Toronto, Ontario, Canada.
[7]The University of Liverpool, Liverpool, UK
[8]Heidelberg University Hospital, Heidelberg, Germany
[9]Mayo Clinic, Rochester, MN, USA
[10]Massachusetts General Hospital, Boston, MA, USA
[11]University of Nebraska Medical Centre, Omaha, NE, US
[12]Molecular Genetics Department, University of Toronto, Toronto, Ontario, Canada
[13]Division of Medical Oncology, Princess Margaret Cancer Centre, Toronto, Ontario, Canada
[14]Department of Pathology, University Health Network, Toronto, Ontario, Canada.
[15]Department of Laboratory Medicine and Pathobiology, University of Toronto, Ontario, Canada.
[16]Department of Medical Biophysics, University of Toronto, Toronto, ON Canada.
[17]BioSpecimen Sciences Program, University Health Network, Toronto, Ontario, Canada.
[18]Theoretical Biology and Biophysics (T-6), Los Alamos National Laboratory, Los Alamos, New Mexico, USA.
[19]Center for Nonlinear Studies, Los Alamos National Laboratory, Los Alamos, New Mexico, USA.

To whom correspondence should be addressed:

Dr. Steven Gallinger, MD, MSc, FRCS
Professor of Surgery
Head, Hepatobiliary/pancreatic Surgical Oncology Program
University Health Network and Mount Sinai Hospital
University of Toronto
Toronto General Hospital
200 Elizabeth St, 10EN, Room 206, Toronto, Ontario
Canada M5G2C4

Email: steven.gallinger@uhn.ca

Word count: 2,953

IMPORTANCE Outcomes for patients with pancreatic ductal adenocarcinoma (PDAC) remain poor. Advances in next-generation sequencing provide a route to therapeutic approaches, and it is hoped that integrating DNA and RNA analysis with clinicopathologic data is a crucial step to design personalized strategies for this lethal disease.

OBJECTIVES To classify PDAC according to distinct mutational processes, and explore their clinical significance.

DESIGN, SETTING AND PARTICIPANTS We performed a retrospective cohort study of resected PDAC, using cases collected between 2008 and 2015 as part of the International Cancer Genome Consortium. The discovery cohort comprised 160 PDAC from 154 patients (148 primary; 12 metastases) that underwent tumor enrichment prior to whole genome (WGS) and RNA sequencing. The replication cohort comprised 95 primary PDAC that underwent WGS and expression microarray on bulk biospecimens.

INTERVENTIONS 144 discovery and 95 replication cohort patients underwent curative-intent surgery and standard peri-operative management. Treatment data for 24 discovery patients who received neoadjuvant, adjuvant or palliative platinum-based chemotherapy were available for analysis.

MAIN OUTCOMES AND MEASURES Somatic mutations accumulate from sequence-specific processes creating signatures detectable by DNA sequencing. Using non-negative matrix factorization, we measured the contribution of each signature to carcinogenesis, and used hierarchical clustering to subtype each cohort. We examined expression of anti-tumor immunity genes across subtypes to uncover biomarkers predictive of response to systemic therapies.

RESULTS Five predominant mutational subtypes were identified that clustered PDAC into four major subtypes: Age Related; Double-strand break repair (DSBR); Mismatch repair (MMR), and

one with unknown etiology (Signature 8). These were replicated and validated. Signatures were faithfully propagated from primaries to matched metastases, implying their stability during carcinogenesis. Half of the DSBR cases lacked germline or somatic events in canonical homologous recombination genes – *BRCA1*, *BRCA2* or *PALB2*. DSBR and MMR subtypes were associated with increased expression of anti-tumor immunity, including activation of CD8+ T-lymphocytes (*GZMA* and *PRF1*) and over-expression of regulatory molecules (*CTLA-4*, *PD-1* and *IDO-1)*, corresponding to higher frequency of somatic mutations and tumor-specific neoantigens.

CONCLUSIONS AND RELEVANCE Signature-based subtyping may guide personalized therapy of PDAC in the context of biomarker-driven prospective trials.

Pancreatic ductal adenocarcinoma (PDAC) has the lowest 5-year overall survival (OS) of any epithelial carcinoma[1]. Randomized trials[2,3] of adjuvant[4] and palliative[5,6] cytotoxic chemotherapies show modest endpoint improvements with considerable attendant toxicities. Targeted agents trialed without biomarker selection, including evofosfamide, PD-L1[7], CTLA-4[8] and *ERBB2*[9] inhibitors, have not improved OS, except for marginal benefit from erlotinib[10-12]. PDAC outcomes will improve with rational molecular subtyping and ensuing directed therapies, as with breast[13] and lung[14] carcinomas. The PDAC exome[15-17] contains four driver genes, *KRAS*, *TP53*, *CDKN2A* and *SMAD4*, and few disturbed pathways that are not translatable into predictive subtypes. Stratification by somatic events, including MYC amplification and specific KRAS mutant codons[17], is not consistently prognostic. Structural variation in 100 genomes[18] identified four PDAC subtypes, with one predictive of platinum chemotherapy response, but progression-free (PFS) and OS were not assessed. Finally, prognostic transcription-based subtypes have been described[19] and refined[20,21], but with neither relation to genomic features nor therapeutic implications.

Cancer genomes accumulate mutations over cell cycles from DNA damage and repair. Analyses of these processes[22,23], informative in other tumors[24-26], have not been comprehensively reported in PDAC. Signatures representative of each process[22] can be quantified per tumor, and the population ~~of tumors~~ subtyped[25] by their relative contributions. Genomic and transcriptomic landscapes of anti-tumor immunity have been systemically explored in other tumor types[23] and predict response to immunotherapies[26,27], however, the character of immune infiltration and its association with mutational signatures has not been studied in PDAC.

We integrated genome, transcriptome and clinicopathologic data from two independent datasets to define four major signature-based PDAC subtypes. These aligned with known

hereditary pancreas cancer predisposition syndromes (HPCSs)[28], were propagated from primary tumors to paired metastases, and differentially expressed anti-tumor immune markers.

METHODS

Whole genome sequencing (WGS) variant calls, RNA sequencing and microarray expression values, clinical information and metadata for discovery and replication cohorts are available from the ICGC data portal[29] (http://dcc.icgc.org). Discovery cohort samples underwent tumor enrichment prior to sequencing. All reads were processed through the same data workflows. Bioinformatics tool names and versions are provided in Supplement One.

RESULTS

Mutational signatures define four principal PDAC subtypes

Our discovery cohort consisted of 148 primary PDAC and 12 metastases from 154 patients that underwent WGS (Figure 1a, eTable 1). For replication, 95 whole PDAC genomes from 95 patients were obtained from the ICGC (eFigure 1, eTable 1).

We identified 11 mutational signatures in our discovery and 12 in our replication genomes using the approach of Alexandrov *et al.*[30], which were merged by shared etiologies into 7 signatures per cohort. Hierarchical clustering by the proportion of single nucleotide variants (SNVs) attributable to each signature (eFigure 2ab) in each cohort independently confirmed four major subtypes: 1) an "Age Related" group dominated by Signatures 1 and 5, attributed to clock-like mutational processes accumulated over cell divisions[31]; 2) a "double strand break repair, DSBR" group characterized by Signature 3, attributed to deficiencies in homologous recombination repair (HRR) of double-strand breaks; 3) a "mismatch repair, MMR" group characterized by Signatures 6, 20 and 26, attributed to defects in DNA MMR; and 4) a group

characterized by Signature 8, of unknown etiology (Figure 1a; eFigure 1). There were two minor groups in both cohorts, one dominated by Signature 17, another by APOBEC. Tumor cellularity and coverage were consistent between subtypes (eFigure 3). Subtype prevalence was equivalent between cohorts (p=0.075, chi-squared).

We verified that signatures associated with their attributed etiologies. The number of SNVs in Signatures 1 and 5 correlated with patient age at diagnosis across all cases ($r_{discovery}$=0.21, $p_{discovery}$=0.0077; $r_{replication}$=0.23, $p_{replication}$=0.03; Pearson's correlation), while total SNVs did not (eFigure 4).

Tumors dysfunctional in HRR rely on non-conservative forms of DSBR, namely single strand annealing, which creates large structural deletions[32,33], and non-homologous end-joining and microhomology-mediated end joining, which create short deletions (3-20 base pairs in length). Consistent with this, DSBR cases had greater numbers of both large structural and short deletions greater than 3 base pairs relative to Age Related cases ($p_{discovery}<3x10^{-9}$ for each; $p_{replication}<3x10^{-4}$; Wilcoxon) (Figure 1a; eFigure 5).

MMR cases had dramatically more SNVs than Age Related cases ($p_{discovery}$=0.0007; Wilcoxon) (Figure 1a). MMR deficiency was verified by immunohistochemistry and a PCR-based assay (eTable 2). Of the four MMR cases, three had germline and one had only somatic mutations in MMR genes (eTable 3). Published frequencies of MMR deficiency in PDAC vary widely[17,34]. Absence of MMR from the replication cohort is likely due to its smaller size. To validate MMR prevalence, we stained a tumor microarray of 370 PDAC from the European Society Group for Pancreatic Cancer (ESPAC)[35-37] for four MMR proteins. Of 342 successfully stained, six were immunodeficient. Assuming discovery, replication and ESPAC cohorts to be unbiased samplings of one population, we infer MMR deficiency prevalence in PDAC to be

1.7% (0.65-2.7%), nearly equal to that of Lynch syndrome in PDAC[38] (eTable 4). Somatic MMR deficiency thus contributes little to PDAC, unlike colorectal[39] and endometrial[40] cancers.

The discovery cohort included 12 metastases – 10 Age Related, 1 DSBR and 1 MMR. Five of these were matched with three primaries and showed faithful propagation of signatures (Figure 1b), including a DSBR pair with a germline *PALB2* mutation. This implies that mutational processes are established early in carcinogenesis and is important for trials where PDAC metastases are more safely biopsied. Paired primaries and metastases were obtained at autopsy from patients who received palliative chemotherapy (eTable 5).

Tiers of DSBR deficiency

Clinical interest in HRR deficiency is growing, with tailored treatment strategies for breast[41] and ovarian[42] cancer. Of 17 discovery DSBR cases, 11 are explained by bi-allelic inactivation of BRCA1, BRCA2 or PALB2. Nine had pathogenic germline mutations with somatic inactivations of the second allele, and two had bi-allelic somatic inactivations (eTable 6). The remaining six were occult, lacking germline or somatic inactivation of canonical HRR genes, referred to as "BRCAness" in the literature[33]. DSBR etiology in the replication cohort was similar, with two germline, two somatic and six BRCAness. We inferred DSBR prevalence in PDAC to be 10.8% (95%CI 7.0-14.7%), comprising 4.4% (1.9-7.0%) germline deficiency, 1.6% (0.04-3.2%) somatic, and 4.8% (2.2-7.5%) BRCAness. This germline frequency is nearly equal to the prevalence of germline BRCA1 or BRCA2 deficiency in PDAC[43], implying PALB2 contributes minimally to PDAC predisposition.

In the amalgamated discovery and replication DSBR cases, the proportion of SNVs attributed to Signature 3 was greater in germline than somatic cases, with BRCAness cases intermediate (Figure 2). The number of SNVs attributed to a mutational process likely increase

with its duration in tumorigenesis[30]. Thus, germline cases may become HRR deficient earlier, while somatic cases become deficient later or sub-clonally, with BRCAness an admixture of both etiologies. This may have implications for therapies targeting HRR deficiency. BRCAness cases also have relatively low numbers of SVs (Figure 2) and may alternatively harbor a mutational process distinct from classical HRR deficiency.

Assuming one or few genes with "two hits" explain the 12 BRCAness cases, we agnostically compared frequencies of bi-allelic inactivation of genes in the DSBR and Age Related tumors of our amalgamated cohorts (Figure 3). We considered only primaries since metastasis-specific events were reported in PDAC[44]. BRCA2 was the only gene preferentially inactivated in the DSBR group (FDR 0.004%).

The idiopathic Signature 8 is similar to Signature 3, with the additional feature of strand bias for C>A substitutions. The latter was reported in PDAC exomes[17] and attributed to smoking, a PDAC risk factor[45], although our data do not support this epidemiologic association (eFigure 6). Signature 8 is also found in breast cancer[30,46], suggested as due to either past activity of transcription-coupled nucleotide excision repair, or to HRR deficiency. Comparison of frequencies of bi-allelic inactivation per gene in Signature 8 with either DSBR or Age Related primary cases revealed no associations (eFigure 7ab). One Signature 8 case bore a germline missense (rs141465583) of uncertain significance in BRCA1 with somatic loss of the wild type allele. This variant is unlikely to impair HRR as overexpression of GFP-fused BRCA1 p.P977L restored the ability of RAD51 to form ionizing radiation-induced foci in U2OS Flp-In cells depleted of endogenous BRCA1 to a similar extent as wild type GFP-BRCA1 (eFigure 8). Thus, occult drivers of BRCAness and Signature 8 were either so heterogeneous that each affects few

cases or not assayed – non-coding, epigenetic, haploinsufficiency of an HRR-pathway gene, exogenous carcinogens.

Mutational signatures are linked to predisposition syndromes

Truncating germline mutations of HPCS genes were found in 16 cases in our discovery cohort, including BRCA1, BRCA2 and PALB2 mutations in 10, MSH2 and MSH6 in 3, ATM in 2 and CDKN2A in 1. There were 7 HPCS carriers in the replication cohort, including 4 BRCA2, 1 PALB2, 1 ATM and 1 PMS2 (eTable 7). Age at diagnosis differed in discovery but not replication donors with, versus without, HPCS ($p_{discovery}$=0.0015, $p_{replication}$=0.32, t-test; eFigure 9).

Most HPCS patients developed tumors driven by processes linked to their predispositions, demonstrating the importance of recognizing HPCS, including genetic counseling and germline testing. A minority developed tumors with processes unrelated to their predisposition. The somatic MMR discovery case had a germline BRCA2 frameshift. Another discovery donor had a germline MSH6 frameshift, but a tumor that was microsatellite stable and strongly positive for Signature 17, of unknown etiology. One replication case had a germline stopgain in PMS2 (not long-range PCR verified) that was microsatellite stable, and two cases had germline BRCA2 truncations without somatic "second hits" that lacked Signature 3. The latter agrees with a mouse model heterozygous for BRCA2 that retained the second, functional allele in PDAC and was not sensitive to mitomycin C and PARP1 inhibitors[47].

Nine discovery and seven replication cases had bi-allelic events in ATM. Only one bore Signature 3, the replication germline ATM carrier who lacked inactivation of another canonical HRR gene (eFigure 10).

225 **Integration of mutational signatures with gene expression**

226 We performed RNASeq on 76 discovery tumors. Our replication cohort had array expression
227 data for 91 cases. We classified these by Collisson et al.[19], Moffitt et al.[20] and Bailey et al.[21]
228 methodologies. As with other cancers, including melanoma[24] and colorectal cancer[48], mutational
229 and transcriptional subtypes did not overlap (eFigure 11). Survival analyses trended towards
230 worse prognosis in the Moffitt basal subtype (eFigure 12).

231 We used gene sets[23] representative of 16 categories of immune function to characterize
232 local immune activity. Adaptive immunity and co-inhibition genes were more highly expressed
233 in DSBR and MMR cases (Figure 4a; eFigure 13a). Cytolytic activity of infiltrating CD8+ T-
234 lymphocytes, measured by the geometric mean of *GZMA* and *PRF1* expression, and co-
235 regulatory molecules, namely CTLA-4, PD-L1, PD-L2 and IDO-1, were increased in DSBR and
236 MMR relative to Age Related cases (eFigure 14), reminiscent of expression patterns in
237 melanoma responsive to checkpoint blockade[49]. Clustering of cases by differential expression of
238 the genes in these sets[23] identified most DSBR (*discovery* 6 of 6 DSBR, *replication* 5 of 8) and
239 all MMR cases as "immunogenic" (eFigure 15-16). The DSBR primary and metastasis pair both
240 had high cytolytic activity, implying anti-tumor responses are driven intrinsically.

241 To relate signatures to elevated cytolytic activity, we enumerated tumor neoantigens in
242 discovery and replication cases. These paralleled SNV counts ($r_{discovery}$=0.98, $p_{discovery}<3x10^{-16}$;
243 $r_{replication}$=0.85, $p_{replication}<3x10^{-16}$; Pearson's) (Figure 4b; eFigure 13b) and were elevated in
244 DSBR and MMR cases ($p_{discovery}=1.8x10^{-7}$; $p_{replication}=2.9x10^{-5}$; DSBR vs. Age Related;
245 Wilcoxon) (eFigure 17). The number of neoantigens per SNV did not differ by subtype, implying
246 no signature was inherently "immunogenic". Neither neoantigen nor SNV counts were
247 associated with OS (eFigure 18). We found no other drivers of anti-tumor immunity, including

incorporation of exogenous viruses, expression of endogenous retroviruses or of cancer testes antigens.

Equal frequencies of bi-allelic mutations in genes in the DSBR and Age Related cases (Figure 3) imply that neither tumor suppressor, nor HLA Class 1, nor extrinsic apoptosis gene inactivation are immune resistance strategies in PDAC.

Cytolytic activity, CD8A and PD-L1 expression strongly correlated with CD8 and PD-L1 immunohistochemistry on a tumor microarray of 33 separate PDAC cases, validating our RNAseq (Figure 5; p-values in legend). Histology from 81 discovery cases showed no difference in the degree of peri- and intra-tumoral inflammation across signature classes, implying microscopy alone cannot accurately measure local anti-tumor immunity (eFigure 19).

Prognostic and predictive value of mutational signatures

Signature groups were neither prognostic nor associated with tumor grade and stage (eFigure 20-21). Favorable outcomes are anecdotally reported for MMR deficient PDAC[50-52]. The four discovery MMR patients had median OS of 1281 days (Q1:Q3 1248-1457 days) compared with 461 (254-1165) for Age-Related cases. The stage IV MMR case is alive 24 months from diagnosis, responding to immunotherapy. In contrast, the 6 MMR immunodeficient ESPAC cases had worse survival than immunointact cases (p=0.03, log-rank test; eFigure 22). Rarity of MMR deficiency precludes definitive conclusions.

Roughly 1 in 10 cases in both cohorts have the DSBR signature. Since HRR deficient PDAC[18], breast[42] and ovarian[41] cancers may be sensitive to platinum-based therapy, we compared outcomes in 18 cases treated with either cisplatin or oxaliplatin (eTable 8; eWorksheet 1). In the palliative setting, median PFS was not significantly longer in DSBR than Age Related cases (181.5 *vs.* 107 days) (eFigure 23). Platinum responders were observed in both groups,

suggesting platinum-based therapy may also benefit non-DSBR cases. Sample size limitations preclude determining whether susceptibility varies with proportion of DSBR.

DISCUSSION

Mutational signatures in WGS defined four major PDAC classes, namely Age Related, DSBR, MMR and Signature 8. These were verified, replicated in independent cohorts, associated with predisposition syndromes and propagated from primary to metastatic lesions. PDAC bearing DSBR and MMR signatures have elevated local anti-tumor immunity, driven by high levels of tumor neoantigens and evaded by expression of regulatory genes. This has implications for personalized management of PDAC.

Approximately 10% of PDAC is categorized as DSBR. Slightly more than half of these have bi-allelic inactivation of HRR genes; the rest are occult. The latter have lower numbers of large and small deletions greater than three base pairs relative to DSBR cases with known causal variants. These BRCAness tumors may have milder HRR deficiency or may represent a novel process that generates DSBR-like nucleotide substitutions but is distinct from classical HRR deficiency at a SV level. We might not expect platinum- or PARP inhibitor-based therapies directed at HRR deficiencies to be as effective in the BRCAness group, nor perhaps in the somatic DSBR cases that have a lower proportion of Signature 3 attributed SNVs. Similarly, ovarian cancers with BRCA1 promoter hypermethylation are less sensitive to chemotherapy than those with BRCA1 mutations[53,54], despite both being HRR deficient. This may explain why exceptional responses to platinum-based chemotherapy are not seen in 10% of PDAC patients in clinical trials. Our failure to retrospectively detect significant improvement in PFS in a palliative setting in DSBR cases is also consistent with heterogeneous mechanisms of HRR deficiency and

295 secondary platinum resistance. Biomarker-driven prospective trials of PARP inhibitors[55] and
296 platinum-based therapies should clarify this controversy.

297 Though BRCAness genomes do not appear to be driven by one or few genes, multiple
298 lines of evidence support the distinction of these cases. At the nucleotide level, the analogous
299 mutational processes acting in germline, somatic and occult DSBR cases give rise to tumor-
300 specific neoantigens that in turn drive anti-tumor cytolytic activity, a prerequisite to successful
301 immunotherapy[23]. A recent study found that metastatic melanoma responding to anti-PD-1
302 therapy are enriched for mutations in BRCA2[56]. The rate of neoantigen formation per SNV was
303 equal across signature types, implying that increased mutation rate alone may predict checkpoint
304 inhibitor response, as shown in colorectal cancer[27], and platinum-based chemotherapy response,
305 as shown in ovarian cancer[57]. While it has been hypothesized that sequestration protects PDAC
306 cells from adaptive immunity[58-60], our data suggest that resistance occurs through increased
307 expression of PD-1, CTLA-4 and IDO-1. The potential for immunotherapy in PDAC has
308 recently been demonstrated in a mouse model that recapitulates its fibrotic stroma using T cells
309 engineered to recognize PDAC-specific antigen[61]. The progressive dysfunction of these T cells
310 in vivo is compatible with our RNA expression findings, implying a role for immune checkpoint
311 inhibition. Also, high expression of IDO-1 in both DSBR and MMR cases argues for trials of
312 IDO-1 inhibitors in PDAC, as in other cancers[62,63]. Current limited success of immunotherapy in
313 PDAC[7,8] may be because only a minority of cases have significant local anti-tumor activity.
314 Nonetheless, our data do not prove responsiveness to immunotherapies in subtypes of PDAC.
315 Other important factors, such as host immunocompetence and tumor microenvironment, must be
316 better understood to facilitate use of immunotherapeutics in clinical settings.

The nature of our cDNA-based RNA capture did not allow assessment of expression of all endogenous retroviruses or cancer testes antigens, nor quantification of tumor cellularity from RNASeq. Tumor cellularity estimates of the same fresh tissue from sections used for WGS were not significantly different between subtypes (eFigure 3). Our outcome analyses are limited by the retrospective nature of this work, including non-randomized patient treatment selection and possible confounding factors not balanced between subtypes. Also, bi-allelic inactivation of other genes important to both DNA damage response and PDAC predisposition, such as ATM[64], were not associated with signatures, implying that either our whole genome sample size was too small to detect all mutational processes or that the contribution of mutations produced by some processes were too few to be detected[30]. Nonetheless, that genomic and transcriptomic data generated separately with different platforms agree in all aspects validates our findings.

Ours and other sequencing efforts have focused on resectable PDAC, constituting a fifth of cases. Improving outcomes for the majority of patients with metastatic disease is sorely needed. Our analysis provides a framework for integrating genomics and transcriptomics to suggest translatable differences between tumor subtypes. We are now applying this to whole genome and transcriptome sequences from tumor biopsies to understand resistance to conventional treatment and to select second-line strategies for patients with advanced disease within the context of a prospective clinical trial (NCT- 02750657).

Figure and Table Captions

Figure 1:
(A) Barplot of proportion of seven merged signatures in each of the 160 discovery tumors, sorted by hierarchical clustering (dendogram at bottom), showing germline (dark blue), somatic (mauve) and occult (clear) DSBR etiologies and heatmaps for total number of single nucleotide variants (SNVs), total number of neoantigens, total number of indels, total number of short deletions greater than 3 base pairs, total number of structural deletions, and transcriptional subtypes (Moffitt Tumor class, Collisson class and Bailey class) in cases for which RNASeq is available for the tumor;
(B) Barplots of proportion of 7 merged signatures in paired primary tumors and metastases from 4 cases.

Figure 2:
Boxplots of proportion of SNVs attributed to Signature 3, number of short deletions greater than 3 base pairs in length, number of SVs, and number of large (structural) deletions in the DSBR subtype divided by etiology – germline (dark blue), BRCAness / occult (clear) or somatic (mauve) – and in the Age Related subtype (light blue), for amalgamated discovery and replication cohorts. All values are significantly greater in both DSBR germline and BRCAness / occult groups relative to the Age Related subtype, $p < 0.0002$ for each, Wilcoxon test, as marked by asterisks.

Figure 3:
Scatterplot of proportions of cases with bi-allelic inactivation of every gene in the DSBR subtype primary tumors (n=27) versus that in the Age Related subtype primary tumors (n=169) for the amalgamated discovery and replication cohorts. Driver genes include *CDKN2A*, *SMAD4*, *TP53*. FDR = false discovery rate

Figure 4:
(A) Heatmap of median expression of gene sets representative of categories of immune function by signature group for discovery cohort cases with tumor cellularities between 20-80%;
(B) Scatterplot of number of neoantigens (y-axis) versus number of somatic SNVs (single nucleotide variants, x-axis) per tumor, colored by signature-based subtype, for 137 discovery cohort cases to which we confidently assigned HLA Class 1 genotypes. Regression line from linear model (y ~ x) is shown in black with areas between confidence bands shaded in grey.

Figure 5:
(A) PD-L1 and CD8 immunohistochemical expression in representative cancer TMA spots showing high (left column) and low (right column) expression of PD-L1 (top row) and CD8 counts (bottom row);
(B) Median (dotted lines) and interquartile ranges (shaded regions) of expression of PD-L1, CD8A and cytolytic activity (left-sided y-axis) and absolute counts of cells with immunohistochemical staining for CD8 (right-sided y-axis) at each level of PD-L1 immunohistochemical staining (0-3, see Methods). CD8 staining cell counts and CD8A expression were strongly correlated ($p = 7.1 \times 10^{-7}$, R 0.744, Pearson's correlation). PD-L1 and cytolytic activity expression were significantly higher across PD-L1 staining levels ($p_{PD\text{-}L1} = 0.0064$, $p_{cytolytic\ activity} = 0.01$, PD-L1 0-1 vs 2-3 staining, Wilcoxon test).

383
384
385

eFigure 1:
Barplot of proportion of seven merged signatures in each of the 95 replication tumors, sorted by hierarchical clustering (dendrogram at bottom), showing germline (blue), somatic (mauve) and occult (clear) DSBR etiologies and heatmaps for total number of SNVs, total number of neoantigens, total number of indels, total number of short deletions greater than 3 base pairs, total number of structural deletions, and transcriptional subtypes (Moffitt Tumor class, Collisson class and Bailey class) in cases for which expression microarray data are available for the tumor.

eFigure 2:
Hierarchical clustering of (A) 160 discovery and (B) 95 replication cohort samples according to proportion (see Figure 1a and eFigure 1) of seven merged signatures in each tumor. Dark green = MMR, dark blue = DSBR, gold = Signature 8, light green = APOBEC, pink = Signature 17, light blue = Age Related

eFigure 3:
Boxplots of (A) & (C) cellularity and (B) & (D) mean tumor coverage by signature-based subtype for (A) & (B) discovery and (C) & (D) replication cohorts

eFigure 4:
Scatterplots of age at surgery versus either (A) & (E) total number of somatic SNVs, (B) & (F) number of SNVs attributed to Age Related signatures, (C) & (G) number of SNVs attributed to Signature 1, (D) & (H) number of SNVs attributed to Signature 5 in (A-D) discovery and (E-H) replication cohorts. Regression lines from linear models (y ~ x) are shown in solid black with areas between confidence bands shaded in grey

eFigure 5:
Boxplots of number of (A) & (G) SVs, (B) & (H) structural (large) deletions, (C) & (I) inversions, (D) & (J) duplications, (E) & (K) transversions, and (F) & (L) short deletions >3 base pairs in tumors of each signature-based subtypes for (A-F) discovery and (G-L) replication cohorts. *P*-values from comparison of numbers of each somatic variant class in DSBR vs Age Related subtypes by Wilcoxon test

eFigure 6:
Smoking status in Age Related ('signature.1.5') and Signature 8 ('signature.8') in (A) discovery and (B) replication cohorts.

eFigure 7:
Scatterplot of frequency of bi-allelic inactivation of every gene in (A) the Signature 8 subtype primary tumors (n=36) versus that in the Age Related subtype primary tumors (n=169) and in (B) the Signature 3 subtype primary tumors (n=27) versus that in the Signature 8 subtype primary tumors (n=36) for the amalgamated discovery and replication cohorts. Driver genes include *CDKN2A*, *SMAD4*, *TP53*. FDR = false discovery rate

eFigure 8:
RAD51 assay performed on BRCA1 p.P977L (rs141465583) germline variant of uncertain significance demonstrates ability of variant allele to restore irradiation-induced foci.

eFigure 9:
Boxplots of (A) age at surgery in discovery cohort, (B) age at diagnosis in replication cohort, and (C) the amalgamated cohorts for those cases with and without pathogenic germline variants in HPCSs genes. *P* values for comparison of ages in Hereditary Pancreas Cancer Syndrome (HPCS) carriers vs non-HPCS carriers are by t-test.

eFigure 10:
Stripcharts of proportion of SNV's attributed to each merged signature in cases with bi-allelic inactivation vs monoallelic inactivation and wild type ATM for the amalgamated discovery and replication cohorts.

eFigure 11:
Proportions of (A,C,E) Moffit tumor and (B,D,F) Collisson transcriptional-based subtypes composed of each signature-based subtype for (A-B) discovery, (C-D) replication and (E-F) combined cohorts.

eFigure 12:
Overall survival curves for (A,D) Moffitt tumor, (B,E) Collisson and (C,F) Bailey transcriptional-based subtypes in (A-B) discovery and (C-D) replication cohorts.

eFigure 13:
(A) Heatmap of median expression of gene sets representative of categories of immune function by signature group for replication cohort cases with tumor cellularities between 20-80%;
(B) Scatterplots of number of neoantigens (y-axis) versus number of somatic SNVs (single nucleotide variants, x-axis) per tumor, colored by signature-based subtype, for 87 replication cohort cases to which we confidently assigned HLA Class 1 genotypes. Regression line from linear model ($y \sim x$) is shown in black with areas between confidence bands shaded in grey.

eFigure 14:
Boxplots of expression of cytolytic activity, CTLA-4, PD-L1, PD-L2 and IDO-1 in signature-based subtypes in discovery (top row) and replication (bottom row) cohort cases with tumor cellularities between 20-80%. The differences in expression between AR (Age Related) and either DSBR or MMR are calculated by Wilcoxon test; FPKM = Fragments Per Kilobase of transcript per Million mapped reads.

eFigure 15:
Heatmap of expression of 113 genes representative of categories of immune function in discovery RNASeq cases with tumor cellularities between 20-80%. Hierarchical clustering shows increased immune activity in all discovery DSBR (6 of 6) and MMR (2 of 2) cases.

eFigure 16:
Heatmap of expression of 113 genes representative of categories of immune function in replication microarray expression cases with tumor cellularities between 20-80%. Hierarchical clustering shows increased immune activity in 5 of 8 DSBR.

eFigure 17:
Boxplots of (A,D) number of neoantigens, (B,E) number of somatic single nucleotide variants (SNV), (C,F) number of neoantigens per SNV in tumors of each signature-based subtypes for (A-C) discovery and (D-F) replication cohorts. *P* values calculated by Wilcoxon test.

eFigure 18:
Overall survival curves with stratification by standard deviation of (A,D) somatic single nucleotide variants (SNV), (B,E) somatic insertion and deletion variants and (C,F) neoantigen load (A-C) discovery and (D-F) replication cohorts.

eFigure 19:
Proportions of tumors divided by (A,C) presence or absence and (B,D) degree of (A-B) intra- and (C-D) peri-tumoral inflammation composed of each signature-based subtype for the discovery cohorts cases with haematoxylin and eosin stained slides available (n = 81).

eFigure 20:
Overall survival curves for signature-based subtypes in (A) discovery and (B) replication cohorts.

eFigure 21:
Proportions of tumors divided by (A) histologic grade, (B) T stage, (C) N stage, (D) M stage composed of each signature-based subtype for (A-D) discovery and (E-H) replication cohorts.

eFigure 22:
Overall survival curve for ESPAC cohort according to mismatch repair protein immunohistochemistry (IHC) deficiency.

eFigure 23:
Progression free survival with stratification by Signature 3 (DSBR) vs Signatures 1+5 (Age Related) for (A) all cases that received platinum-based palliative chemotherapy and (B) all cases that responded to platinum-based palliative chemotherapy. *P* values by univariable Cox proportional hazard models.

eTable 1:
Summary of clinical and pathologic data for discovery and replication cohorts with appropriate statistical comparisons between the two groups.

eTable 2:
Summary of immunohistochemistry of 4 MMR proteins and PCR-based microsatellite instability testing for discovery cohort. Acronyms: MSS = microsatellite stable; MSI = microsatellite instability; NA = not available

eTable 3:
Summary of germline and somatic mutations in hereditary pancreatic cancer syndrome (HPCS) genes in cases whose tumors had mismatch repair deficiency in the discovery cohort.

eTable 4:
Number of cases per signature-based subtype per cohort and derived population-level estimates.

eTable 5:
Summary of clinical and pathologic data, including palliative chemotherapy regimens, received by cases with paired primaries and tumours (for signatures, see Figure 1B).

eTable 6a,b:
Summary of germline and somatic mutations in BRCA1, BRCA2 and PALB2 in cases whose tumors have evidence of double strand break repair deficiency in discovery and replication cohorts. Acronym: LOH = loss of heterozygosity of the wild type allele of the affected gene

eTable 7a,b:
Summary of pathogenic germline variants in hereditary pancreatic cancer syndrome (HPCS) genes in discovery and replication cohorts.

eTable 8:
Summary of cases that received platinum-based palliative chemotherapy in the discovery cohort; see Supplement One for statistical methodologies.

eWorksheet 1:
Treatment details of cases that received platinum-based palliative chemotherapy in the discovery cohort; see Supplement One for further details.

Acknowledgements

This study was conducted with the support of the Ontario Institute for Cancer Research (PanCuRx Translational Research Initiative) through funding provided by the Government of Ontario (Ministry of Research and Innovation); the Canada Foundation for Innovation; Pancreas Cancer Canada; NCI grant P50 CA102701 (Mayo Clinic SPORE in Pancreatic Cancer), a Canadian Cancer Society Research Institute grant (#702316), and a charitable donation from the Canadian Friends of the Hebrew University (Alex U. Soyka). FN is supported by a fellowship award from the Canadian Institutes for Health Research (CIHR). LDS, JDM, VF, PB, BW and SG are recipients of Fellowships, Investigator or Clinician-Scientist Awards from the Ontario Institute for Cancer Research. DD was supported by CIHR grant MOP-84297. The ESPAC Trials and the Liverpool Cancer Trials Unit are funded by Cancer Research UK. JPN is a Senior NIHR Investigator.

AAC, RED, GHJ, SNK, GW, MACSY, VF, JPN, MB, DD, PB, LBA, FN, LDS and SG conducted and are responsible for the data analysis. LDS had full access to all of the data in the study and takes responsibility for the integrity of the data and the accuracy of the data analysis.

We acknowledge the technical contributions of the following individuals for their roles in Production Sequencing and Genome Sequence Informatics at the Ontario Institute for Cancer Research: Karolina Czajka, Jenna Eagles, Jeremy Johns, Xuemei Luo, Faridah Mbabaali, Jessica Miller, Danielle Pasternack, Michelle Sam, Morgan Taschuk, as well as the contributions of Dianne Chadwick, Sheng-Ben Liang and Sagedeh Shahabi at the University Health Network BioBank.

JPN has the following declarations:
Payment for Lectures: Amgen, Mylan
Research Grants: Taiho Pharma (Japan); KAEL GemVax (Korea); AstraZeneca; Clovis Oncology and Ventana; Pharma Nord
Consultancy: Boehringer Ingelheim Pharma GmbH & Co. KG; Novartis Pharma AG; KAEL GemVax; Astellas
Educational Travel Grants: NUCANA

References Cited

1 National Cancer Institute. Surveillance, Epidemiology and End Results Program. http://seer.cancer.gov/statfacts/html/pancreas.html).

2 Kalser, M. H. & Ellenberg, S. S. Pancreatic cancer. Adjuvant combined radiation and chemotherapy following curative resection. *Archives of surgery* **120**, 899-903 (1985).

3 Oettle, H. *et al.* Adjuvant chemotherapy with gemcitabine and long-term outcomes among patients with resected pancreatic cancer: the CONKO-001 randomized trial. *Jama* **310**, 1473-1481, doi:10.1001/jama.2013.279201 (2013).

4 Garrido-Laguna, I. & Hidalgo, M. Pancreatic cancer: from state-of-the-art treatments to promising novel therapies. *Nature reviews. Clinical oncology* **12**, 319-334, doi:10.1038/nrclinonc.2015.53 (2015).

5 Von Hoff, D. D. *et al.* Increased survival in pancreatic cancer with nab-paclitaxel plus gemcitabine. *The New England journal of medicine* **369**, 1691-1703, doi:10.1056/NEJMoa1304369 (2013).

6 Conroy, T. *et al.* FOLFIRINOX versus gemcitabine for metastatic pancreatic cancer. *The New England journal of medicine* **364**, 1817-1825, doi:10.1056/NEJMoa1011923 (2011).

7 Brahmer, J. R. *et al.* Safety and activity of anti-PD-L1 antibody in patients with advanced cancer. *The New England journal of medicine* **366**, 2455-2465, doi:10.1056/NEJMoa1200694 (2012).

8 Royal, R. E. *et al.* Phase 2 trial of single agent Ipilimumab (anti-CTLA-4) for locally advanced or metastatic pancreatic adenocarcinoma. *Journal of immunotherapy* **33**, 828-833, doi:10.1097/CJI.0b013e3181eec14c (2010).

9 Harder, J. *et al.* Multicentre phase II trial of trastuzumab and capecitabine in patients with HER2 overexpressing metastatic pancreatic cancer. *Br J Cancer* **106**, 1033-1038, doi:10.1038/bjc.2012.18 (2012).

10 Moore, M. J. *et al.* Erlotinib plus gemcitabine compared with gemcitabine alone in patients with advanced pancreatic cancer: a phase III trial of the National Cancer Institute of Canada Clinical Trials Group. *Journal of clinical oncology : official journal of the American Society of Clinical Oncology* **25**, 1960-1966, doi:10.1200/JCO.2006.07.9525 (2007).

11 da Cunha Santos, G. *et al.* Molecular predictors of outcome in a phase 3 study of gemcitabine and erlotinib therapy in patients with advanced pancreatic cancer: National Cancer Institute of Canada Clinical Trials Group Study PA.3. *Cancer* **116**, 5599-5607, doi:10.1002/cncr.25393 (2010).

12 Kim, S. T. *et al.* Impact of KRAS mutations on clinical outcomes in pancreatic cancer patients treated with first-line gemcitabine-based chemotherapy. *Molecular cancer therapeutics* **10**, 1993-1999, doi:10.1158/1535-7163.MCT-11-0269 (2011).

13 Prat, A. *et al.* Clinical implications of the intrinsic molecular subtypes of breast cancer. *Breast* **24 Suppl 2**, S26-35, doi:10.1016/j.breast.2015.07.008 (2015).

14 Devarakonda, S., Morgensztern, D. & Govindan, R. Genomic alterations in lung adenocarcinoma. *The Lancet. Oncology* **16**, e342-351, doi:10.1016/S1470-2045(15)00077-7 (2015).

15 Biankin, A. V. *et al.* Pancreatic cancer genomes reveal aberrations in axon guidance pathway genes. *Nature* **491**, 399-405, doi:10.1038/nature11547 (2012).

16 Jones, S. *et al.* Core signaling pathways in human pancreatic cancers revealed by global genomic analyses. *Science* **321**, 1801-1806, doi:10.1126/science.1164368 (2008).

17 Witkiewicz, A. K. *et al.* Whole-exome sequencing of pancreatic cancer defines genetic diversity and therapeutic targets. *Nature communications* **6**, 6744, doi:10.1038/ncomms7744 (2015).

18 Waddell, N. *et al.* Whole genomes redefine the mutational landscape of pancreatic cancer. *Nature* **518**, 495-501, doi:10.1038/nature14169 (2015).

19 Collisson, E. A. *et al.* Subtypes of pancreatic ductal adenocarcinoma and their differing responses to therapy. *Nature medicine* **17**, 500-503, doi:10.1038/nm.2344 (2011).

20 Moffitt, R. A. *et al.* Virtual microdissection identifies distinct tumor- and stroma-specific subtypes of pancreatic ductal adenocarcinoma. *Nature genetics* **47**, 1168-1178, doi:10.1038/ng.3398 (2015).

21 Bailey, P. *et al.* Genomic analyses identify molecular subtypes of pancreatic cancer. *Nature* **531**, 47-52, doi:10.1038/nature16965 (2016).

22 Alexandrov, L. B. *et al.* Signatures of mutational processes in human cancer. *Nature* **500**, 415-421, doi:10.1038/nature12477 (2013).

23 Rooney, M. S., Shukla, S. A., Wu, C. J., Getz, G. & Hacohen, N. Molecular and genetic properties of tumors associated with local immune cytolytic activity. *Cell* **160**, 48-61, doi:10.1016/j.cell.2014.12.033 (2015).

24 Cancer Genome Atlas, N. Genomic Classification of Cutaneous Melanoma. *Cell* **161**, 1681-1696, doi:10.1016/j.cell.2015.05.044 (2015).

25 Schulze, K. *et al.* Exome sequencing of hepatocellular carcinomas identifies new mutational signatures and potential therapeutic targets. *Nature genetics* **47**, 505-511, doi:10.1038/ng.3252 (2015).

26 Van Allen, E. M. *et al.* Genomic correlates of response to CTLA-4 blockade in metastatic melanoma. *Science* **350**, 207-211, doi:10.1126/science.aad0095 (2015).

27 Le, D. T. *et al.* PD-1 Blockade in Tumors with Mismatch-Repair Deficiency. *The New England journal of medicine* **372**, 2509-2520, doi:10.1056/NEJMoa1500596 (2015).

28 Connor, A. A. & Gallinger, S. Hereditary Pancreatic Cancer Syndromes. *Surgical oncology clinics of North America* **24**, 733-764, doi:10.1016/j.soc.2015.06.007 (2015).

29 ICGC Data Portal. https://dcc.icgc.org/).

30 Alexandrov, L. B., Nik-Zainal, S., Wedge, D. C., Campbell, P. J. & Stratton, M. R. Deciphering signatures of mutational processes operative in human cancer. *Cell reports* **3**, 246-259, doi:10.1016/j.celrep.2012.12.008 (2013).

31 Alexandrov, L. B. *et al.* Clock-like mutational processes in human somatic cells. *Nature genetics* **47**, 1402-1407, doi:10.1038/ng.3441 (2015).

32 Ciccia, A. & Elledge, S. J. The DNA damage response: making it safe to play with knives. *Molecular cell* **40**, 179-204, doi:10.1016/j.molcel.2010.09.019 (2010).

33 Lord, C. J. & Ashworth, A. BRCAness revisited. *Nature reviews. Cancer* **16**, 110-120, doi:10.1038/nrc.2015.21 (2016).

34 Riazy, M. *et al.* Mismatch repair status may predict response to adjuvant chemotherapy in resectable pancreatic ductal adenocarcinoma. *Modern pathology : an official journal of the United States and Canadian Academy of Pathology, Inc* **28**, 1383-1389, doi:10.1038/modpathol.2015.89 (2015).

35 Neoptolemos, J. P. *et al.* Adjuvant chemoradiotherapy and chemotherapy in resectable pancreatic cancer: a randomised controlled trial. *Lancet* **358**, 1576-1585 (2001).

36 Neoptolemos, J. P. *et al.* A randomized trial of chemoradiotherapy and chemotherapy after resection of pancreatic cancer. *The New England journal of medicine* **350**, 1200-1210, doi:10.1056/NEJMoa032295 (2004).

37 Neoptolemos, J. P. *et al.* Adjuvant chemotherapy with fluorouracil plus folinic acid vs gemcitabine following pancreatic cancer resection: a randomized controlled trial. *Jama* **304**, 1073-1081, doi:10.1001/jama.2010.1275 (2010).

38 Grant, R. C. *et al.* Prevalence of germline mutations in cancer predisposition genes in patients with pancreatic cancer. *Gastroenterology* **148**, 556-564, doi:10.1053/j.gastro.2014.11.042 (2015).

39 Cancer Genome Atlas, N. Comprehensive molecular characterization of human colon and rectal cancer. *Nature* **487**, 330-337, doi:10.1038/nature11252 (2012).

40 Cancer Genome Atlas Research, N. *et al.* Integrated genomic characterization of endometrial carcinoma. *Nature* **497**, 67-73, doi:10.1038/nature12113 (2013).

41 Muggia, F. & Safra, T. 'BRCAness' and its implications for platinum action in gynecologic cancer. *Anticancer research* **34**, 551-556 (2014).

42 Bayraktar, S. & Gluck, S. Systemic therapy options in BRCA mutation-associated breast cancer. *Breast cancer research and treatment* **135**, 355-366, doi:10.1007/s10549-012-2158-6 (2012).

43 Holter, S. *et al.* Germline BRCA Mutations in a Large Clinic-Based Cohort of Patients With Pancreatic Adenocarcinoma. *Journal of clinical oncology : official journal of the American Society of Clinical Oncology* **33**, 3124-3129, doi:10.1200/JCO.2014.59.7401 (2015).

44 Campbell, P. J. *et al.* The patterns and dynamics of genomic instability in metastatic pancreatic cancer. *Nature* **467**, 1109-1113, doi:10.1038/nature09460 (2010).

45 Bosetti, C. *et al.* Cigarette smoking and pancreatic cancer: an analysis from the International Pancreatic Cancer Case-Control Consortium (Panc4). *Annals of oncology : official journal of the European Society for Medical Oncology / ESMO* **23**, 1880-1888, doi:10.1093/annonc/mdr541 (2012).

46 Nik-Zainal, S. *et al.* Landscape of somatic mutations in 560 breast cancer whole-genome sequences. *Nature*, doi:10.1038/nature17676 (2016).

47 Skoulidis, F. *et al.* Germline Brca2 heterozygosity promotes Kras(G12D) -driven carcinogenesis in a murine model of familial pancreatic cancer. *Cancer cell* **18**, 499-509, doi:10.1016/j.ccr.2010.10.015 (2010).

48 Guinney, J. *et al.* The consensus molecular subtypes of colorectal cancer. *Nature medicine* **21**, 1350-1356, doi:10.1038/nm.3967 (2015).

49 Van Allen, E. M. *et al.* Genomic correlates of response to CTLA-4 blockade in metastatic melanoma. *Science* **350**, 207-211, doi:10.1126/science.aad0095 (2015).

50 Banville, N. *et al.* Medullary carcinoma of the pancreas in a man with hereditary nonpolyposis colorectal cancer due to a mutation of the MSH2 mismatch repair gene. *Human pathology* **37**, 1498-1502, doi:10.1016/j.humpath.2006.06.024 (2006).

51 Goggins, M. *et al.* Pancreatic adenocarcinomas with DNA replication errors (RER+) are associated with wild-type K-ras and characteristic histopathology. Poor differentiation, a syncytial growth pattern, and pushing borders suggest RER+. *The American journal of pathology* **152**, 1501-1507 (1998).

52 Wilentz, R. E. *et al.* Genetic, immunohistochemical, and clinical features of medullary carcinoma of the pancreas: A newly described and characterized entity. *The American journal of pathology* **156**, 1641-1651, doi:10.1016/S0002-9440(10)65035-3 (2000).

53 Cancer Genome Atlas Research, N. Integrated genomic analyses of ovarian carcinoma. *Nature* **474**, 609-615, doi:10.1038/nature10166 (2011).

54 Ruscito, I. *et al.* BRCA1 gene promoter methylation status in high-grade serous ovarian cancer patients--a study of the tumour Bank ovarian cancer (TOC) and ovarian cancer diagnosis consortium (OVCAD). *European journal of cancer* **50**, 2090-2098, doi:10.1016/j.ejca.2014.05.001 (2014).

55 ASCO University. http://meetinglibrary.asco.org/content/147076-156).

56 Hugo, W. *et al.* Genomic and Transcriptomic Features of Response to Anti-PD-1 Therapy in Metastatic Melanoma. *Cell* **165**, 35-44, doi:10.1016/j.cell.2016.02.065 (2016).

57 Birkbak, N. J. *et al.* Tumor mutation burden forecasts outcome in ovarian cancer with BRCA1 or BRCA2 mutations. *PloS one* **8**, e80023, doi:10.1371/journal.pone.0080023 (2013).

58 Jacobetz, M. A. *et al.* Hyaluronan impairs vascular function and drug delivery in a mouse model of pancreatic cancer. *Gut* **62**, 112-120, doi:10.1136/gutjnl-2012-302529 (2013).
59 Olive, K. P. *et al.* Inhibition of Hedgehog signaling enhances delivery of chemotherapy in a mouse model of pancreatic cancer. *Science* **324**, 1457-1461, doi:10.1126/science.1171362 (2009).
60 Provenzano, P. P. *et al.* Enzymatic targeting of the stroma ablates physical barriers to treatment of pancreatic ductal adenocarcinoma. *Cancer cell* **21**, 418-429, doi:10.1016/j.ccr.2012.01.007 (2012).
61 Stromnes, I. M. *et al.* T Cells Engineered against a Native Antigen Can Surmount Immunologic and Physical Barriers to Treat Pancreatic Ductal Adenocarcinoma. *Cancer cell* **28**, 638-652, doi:10.1016/j.ccell.2015.09.022 (2015).
62 Jiang, T. *et al.* Research progress of indoleamine 2,3-dioxygenase inhibitors. *Future medicinal chemistry* **7**, 185-201, doi:10.4155/fmc.14.151 (2015).
63 Zhai, L. *et al.* Molecular Pathways: Targeting IDO1 and Other Tryptophan Dioxygenases for Cancer Immunotherapy. *Clinical cancer research : an official journal of the American Association for Cancer Research* **21**, 5427-5433, doi:10.1158/1078-0432.CCR-15-0420 (2015).
64 Roberts, N. J. *et al.* ATM mutations in patients with hereditary pancreatic cancer. *Cancer discovery* **2**, 41-46, doi:10.1158/2159-8290.CD-11-0194 (2012).

Figure 1

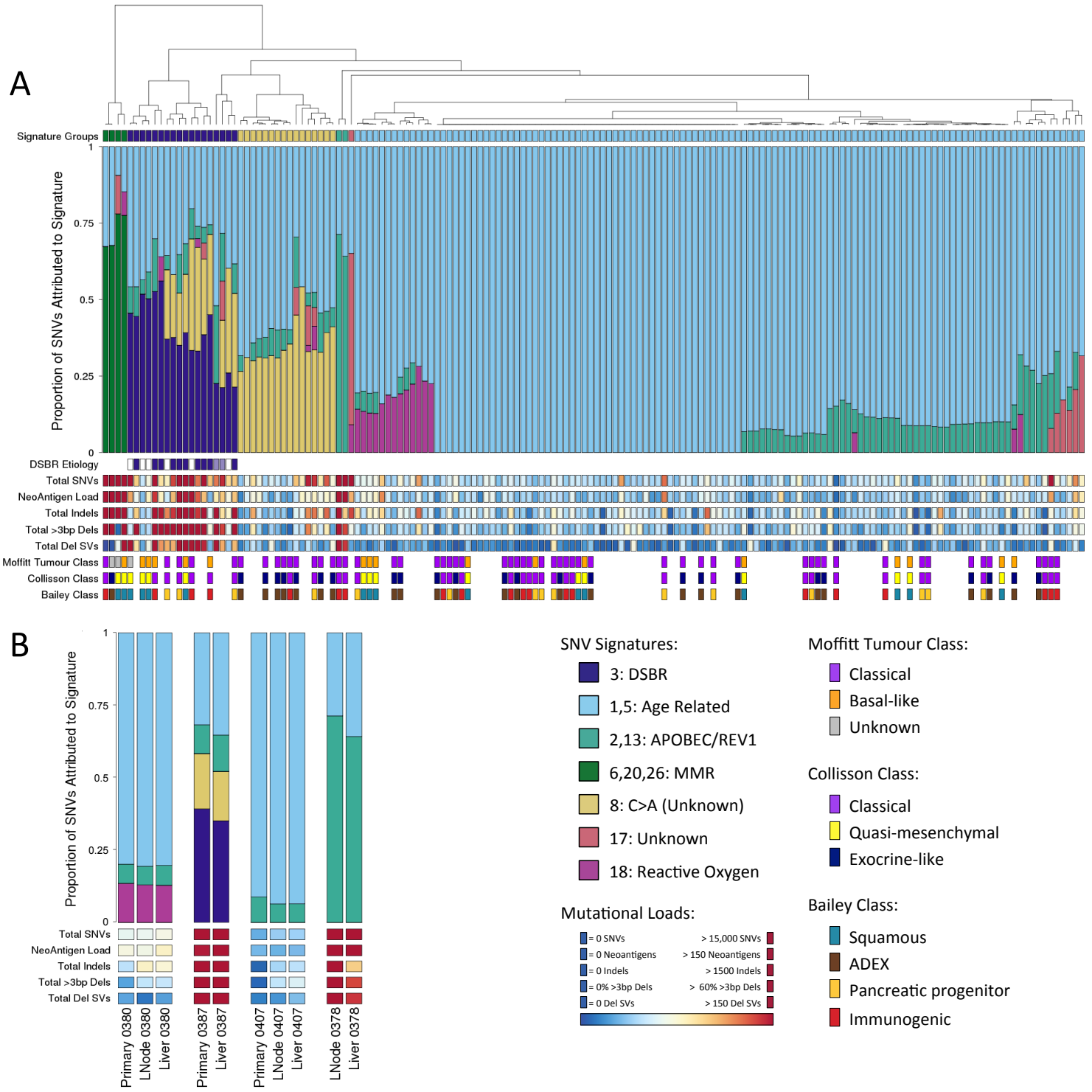
A
Signature Groups
Proportion of SNVs Attributed to Signature
1
0.75
0.5
0.25
0
DSBR Etiology
Total SNVs
NeoAntigen Load
Total Indels
Total >3bp Dels
Total Del SVs
Moffitt Tumour Class
Collisson Class
Bailey Class
B
Proportion of SNVs Attributed to Signature
Total SNVs
NeoAntigen Load
Total Indels
Total >3bp Dels
Total Del SVs
Primary 0380
LNode 0380
Liver 0380
Primary 0387
Liver 0387
Primary 0407
LNode 0407
Liver 0407
LNode 0378
Liver 0378
SNV Signatures:
3: DSBR
1,5: Age Related
2,13: APOBEC/REV1
6,20,26: MMR
8: C>A (Unknown)
17: Unknown
18: Reactive Oxygen
Mutational Loads:
= 0 SNVs
> 15,000 SNVs
= 0 Neoantigens
> 150 Neoantigens
= 0 Indels
> 1500 Indels
= 0% >3bp Dels
> 60% >3bp Dels
= 0 Del SVs
> 150 Del SVs
Moffitt Tumour Class:
Classical
Basal-like
Unknown
Collisson Class:
Classical
Quasi-mesenchymal
Exocrine-like
Bailey Class:
Squamous
ADEX
Pancreatic progenitor
Immunogenic

Figure 2

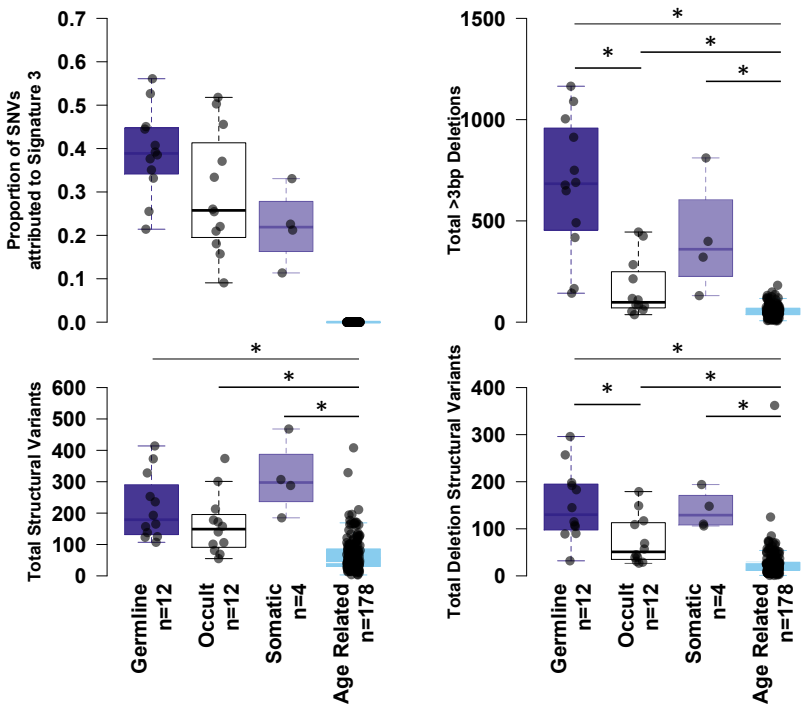
Proportion of SNVs attributed to Signature 3
0.7
0.6
0.5
0.4
0.3
0.2
0.1
0.0
Total >3bp Deletions
1500
1000
500
0
Total Structural Variants
600
500
400
300
200
100
0
Total Deletion Structural Variants
400
300
200
100
0
*
Germline n=12
Occult n=12
Somatic n=4
Age Related n=178

Figure 3

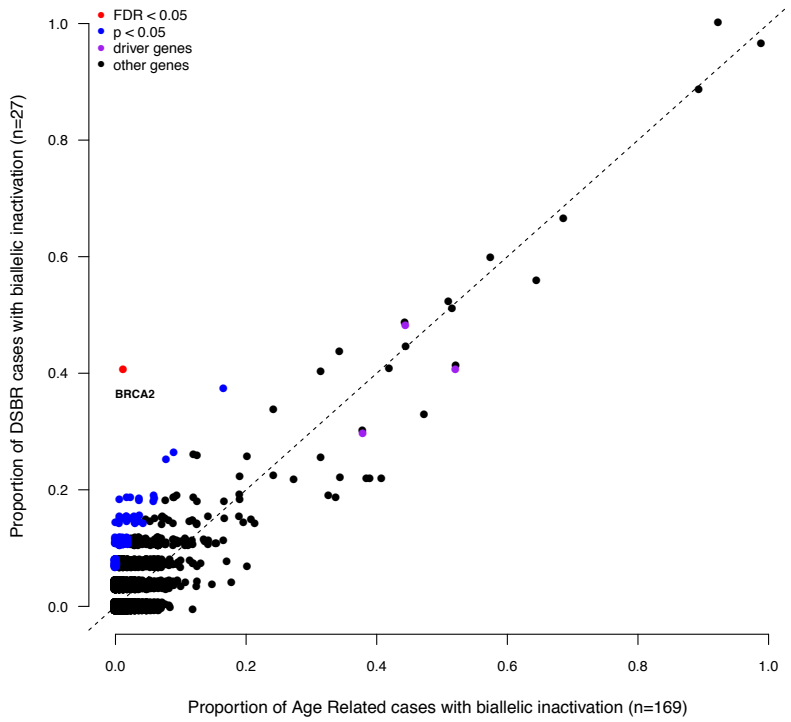
FDR < 0.05
p < 0.05
driver genes
other genes
BRCA2
Proportion of DSBR cases with biallelic inactivation (n=27)
Proportion of Age Related cases with biallelic inactivation (n=169)
0.0
0.2
0.4
0.6
0.8
1.0

Figure 4

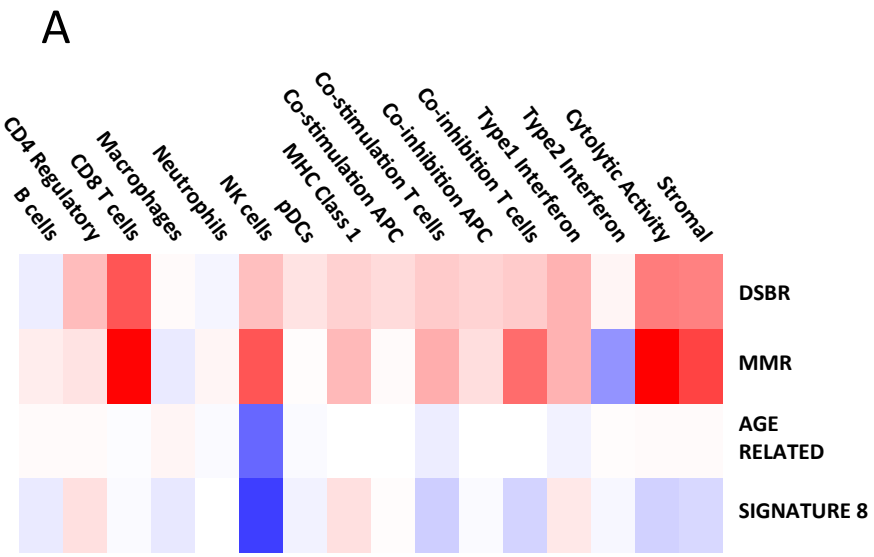
A
B cells
CD4 Regulatory
CD8 T cells
Macrophages
Neutrophils
NK cells
pDCs
MHC Class 1
Co-stimulation APC
Co-stimulation T cells
Co-inhibition APC
Co-inhibition T cells
Type1 Interferon
Type2 Interferon
Cytolytic Activity
Stromal
DSBR
MMR
AGE RELATED
SIGNATURE 8

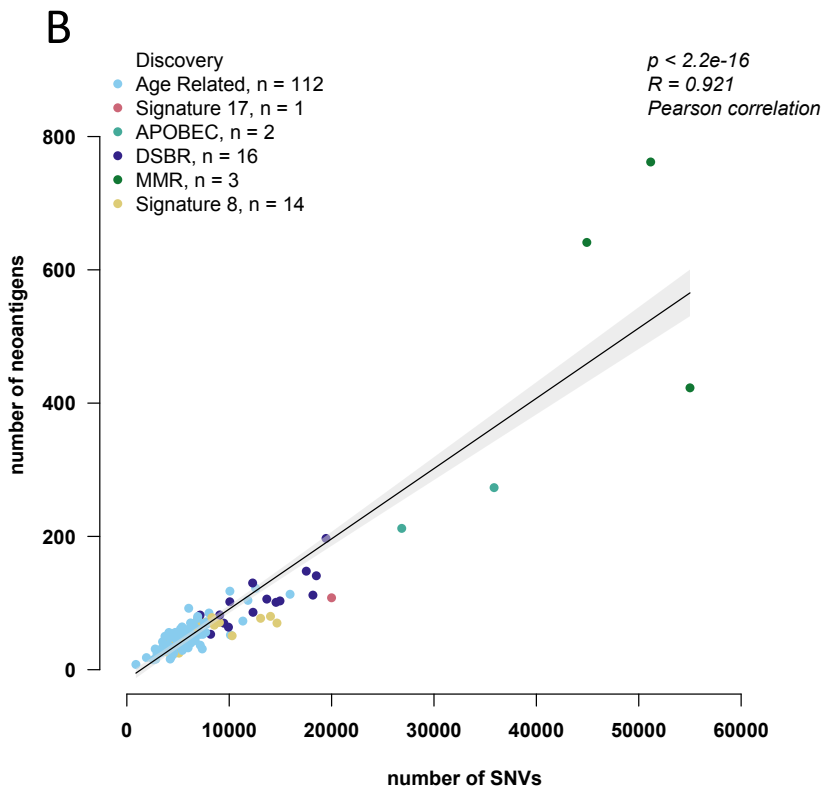
B
Discovery
Age Related, n = 112
Signature 17, n = 1
APOBEC, n = 2
DSBR, n = 16
MMR, n = 3
Signature 8, n = 14
p < 2.2e-16
R = 0.921
Pearson correlation
number of neoantigens
0
200
400
600
800
0
10000
20000
30000
40000
50000
60000
number of SNVs

Figure 5

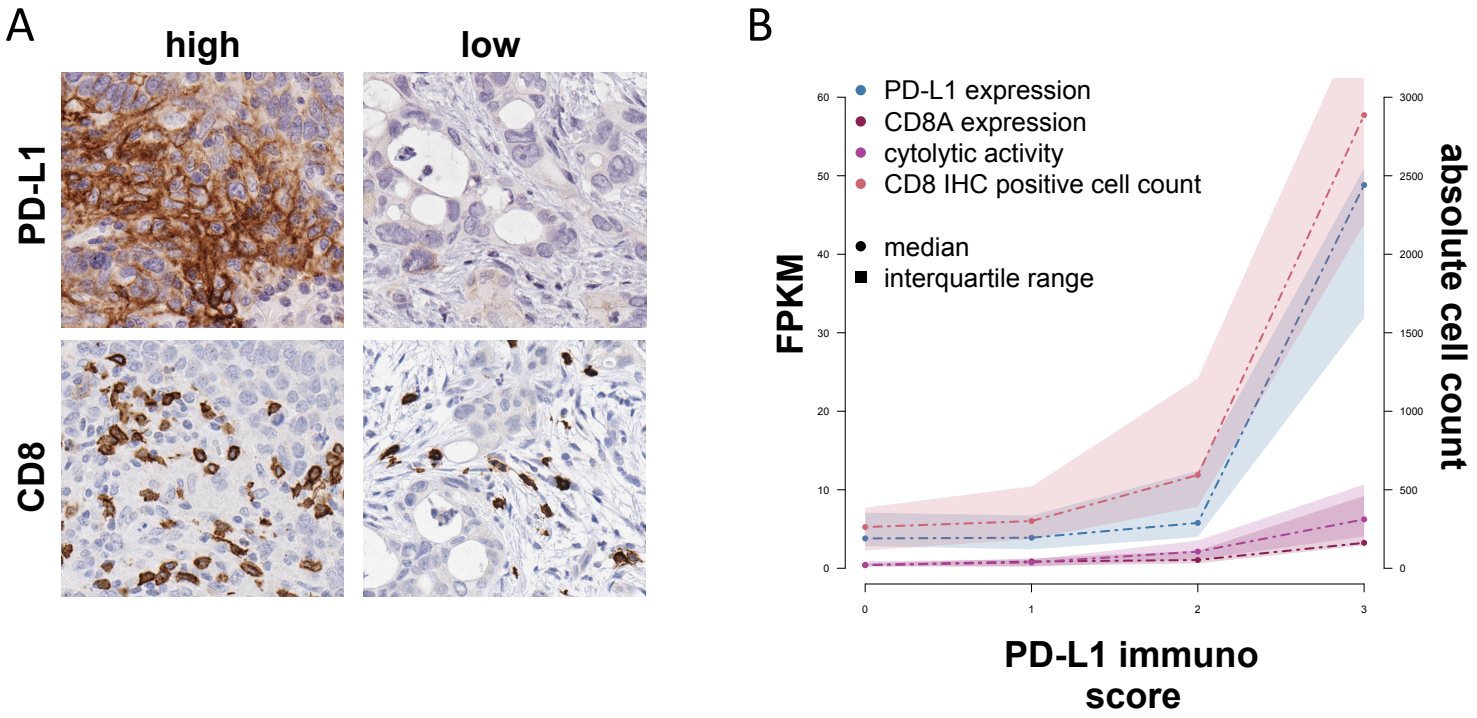
A
high
low
PD-L1
CD8
B
PD-L1 expression
CD8A expression
cytolytic activity
CD8 IHC positive cell count
median
interquartile range
FPKM
absolute cell count
PD-L1 immuno score
0
10
20
30
40
50
60
0
500
1000
1500
2000
2500
3000
0
1
2
3